AIP | APL Materials
NOW INDEXED IN THOMSON REUTERS DATABASES

Research Update: Stoichiometry controlled oxide thin film growth by pulsed laser deposition

Rik Groenen, Jasper Smit, Kasper Orsel, Arturas Vailionis, Bert Bastiaens, Mark Huijben, Klaus Boller, Guus Rijnders, and Gertjan Koster

Citation: APL Materials **3**, 070701 (2015); doi: 10.1063/1.4926933
View online: http://dx.doi.org/10.1063/1.4926933
View Table of Contents: http://scitation.aip.org/content/aip/journal/aplmater/3/7?ver=pdfcov
Published by the AIP Publishing

Articles you may be interested in
Influence of the oxidation state of SrTiO3 plasmas for stoichiometric growth of pulsed laser deposition films identified by laser induced fluorescence
APL Mat. **3**, 106103 (2015); 10.1063/1.4933217

Stoichiometry control of complex oxides by sequential pulsed-laser deposition from binary-oxide targets
Appl. Phys. Lett. **106**, 131601 (2015); 10.1063/1.4916948

Growth diagram of La0.7Sr0.3MnO3 thin films using pulsed laser deposition
J. Appl. Phys. **113**, 234301 (2013); 10.1063/1.4811187

Improved stoichiometry and misfit control in perovskite thin film formation at a critical fluence by pulsed laser deposition
Appl. Phys. Lett. **87**, 241919 (2005); 10.1063/1.2146069

Synthesis and structural, electrochromic characterization of pulsed laser deposited vanadium oxide thin films
J. Vac. Sci. Technol. A **19**, 887 (2001); 10.1116/1.1359533

AIP | APL Photonics
APL Photonics is pleased to announce Benjamin Eggleton as its Editor-in-Chief

This article is copyrighted as indicated in the article. Reuse of AIP content is subject to the terms at: http://aplmaterials.aip.org/about/rights_and_permissions Downloaded to IP: 130.89.45.179 On: Wed, 28 Oct 2015 08:42:35

APL MATERIALS 3, 070701 (2015)

Research Update: Stoichiometry controlled oxide thin film growth by pulsed laser deposition

Rik Groenen, Jasper Smit, Kasper Orsel, Arturas Vailionis, Bert Bastiaens, Mark Huijben, Klaus Boller, Guus Rijnders, and Gertjan Koster[a]
Faculty of Science and Technology and MESA+ Institute for Nanotechnology, University of Twente, 7500 AE Enschede, The Netherlands

(Received 1 May 2015; accepted 30 June 2015; published online 23 July 2015)

The oxidation of species in the plasma plume during pulsed laser deposition controls both the stoichiometry as well as the growth kinetics of the deposited $SrTiO_3$ thin films, instead of the commonly assumed mass distribution in the plasma plume and the kinetic energy of the arriving species. It was observed by X-ray diffraction that $SrTiO_3$ stoichiometry depends on the composition of the background gas during deposition, where in a relative small pressure range between 10^{-2} mbars and 10^{-1} mbars oxygen partial pressure, the resulting film becomes fully stoichiometric. Furthermore, upon increasing the oxygen (partial) pressure, the growth mode changes from 3D island growth to a 2D layer-by-layer growth mode as observed by reflection high energy electron diffraction. © *2015 Author(s). All article content, except where otherwise noted, is licensed under a Creative Commons Attribution 3.0 Unported License.* [http://dx.doi.org/10.1063/1.4926933]

Oxide materials having a perovskite-type crystal structure are widely studied for their broad range of properties and are considered to have great potential for electronic and energy-related applications. For example, it has been shown that perovskite $SrTiO_3$ exhibits a wide range of interesting properties such as ferroelectricity, superconductivity, resistive switching, and thermoelectricity. For this material, these properties are often related to impurity doping,[1] strain,[2] and/or an imperfect or defective crystal, where the properties of the latter are mostly determined by (high) concentrations of oxygen vacancies allowed by the stability of $SrTiO_3$ under reducing conditions due to the multivalency[3] of Ti. Because of the relatively weak binding of the oxygen and the high oxygen-ion mobility, vacancies can be introduced by annealing at low pressures ($<10^{-5}$ mbars). $SrTiO_3$ crystals and thin films can be fabricated with varying oxygen vacancy concentrations, which will transform the wide bandgap insulator into a good conductor. However, besides oxygen vacancies, these properties can also strongly relate to the cation stoichiometry of $SrTiO_3$ where even marginal compositional variations lead to changes in electrical, dielectric, and thermal properties.[4–6]

Besides its interesting properties, $SrTiO_3$ is widely used as model material system for fundamental studies on the influence of growth parameters on oxide thin film characteristics such as crystal structure and surface morphology.[4,7,8] This is because of its simple ABO_3 cubic (A, B being metal cations) perovskite structure as well as the possibility of homoepitaxial growth. Here, thermodynamic factors such as lattice misfit can be excluded and the growth can be described entirely kinetically, which is the basis of the current models describing pulsed laser deposition (PLD) growth processes.[9,10]

In many studies of these kinetic processes on the effect of oxygen (partial) pressures, the unavoidable variations in oxygen stoichiometry could be "repaired" by a simple post-annealing procedure. On the other hand, any resulting variations in cation stoichiometry cannot be corrected afterwards and therefore, a full control of the properties demands tuning of the cation stoichiometry during the thin film growth processing. Most importantly, accurate PLD synthesis requires detailed

[a]Electronic mail: g.koster@utwente.nl

 ©Author(s) 2015

This article is copyrighted as indicated in the article. Reuse of AIP content is subject to the terms at: http://aplmaterials.aip.org/about/rights_and_permissions Downloaded to IP: 130.89.45.179 On: Wed, 28 Oct 2015 08:42:35

knowledge on the relation between plasma plume characteristics and the obtained thin film cation stoichiometry. The laser fluence and the background gas pressure influence the plasma plume and have been previously reported to modify the (homo)epitaxial growth[11,12] of $SrTiO_3$.

A complex ablation process was suggested for a single crystal $SrTiO_3$ target, where it was shown that the composition of the $SrTiO_3$ films changes immediately when the laser fluence is reduced below a certain threshold[13] even though congruent melting takes place. This emphasised the importance of having a high control over the uniformity of the laser intensity at the target as well as the pulse to pulse stability. From this work, an ablation fluence of 1.3 J/cm^2 is suggested, which is a widely used standard. Others observed a correlation between the laser fluence and the out-of-plane lattice constant of the crystal structure[7,14] in which a variation of lattice defects and cation nonstoichiometry resulted in a lattice expansion. They concluded that instead of a threshold, a specific optimal value for the laser fluence exists.

The role of the background pressure on the plasma is often related to the effect of background gas on the kinetic propagation characteristics of the expanding plasma plume.[15] The relation between the characteristics of the expanding plasma plume and the growth parameters has been studied and led to a kinetic model for the pressure dependent propagation dynamics, with a change of the propagation behaviour from thermalised to drag to ballistic. Most importantly, for a typical target to substrate distance of 50 mm, this change occurs within a narrow pressure range from 10^{-2} to 10^{-1} mbars.[16,17] Subsequently, an enhanced film smoothness was correlated to this increased kinetic energy of species at lower background gas pressure.[11,18–20]

Here, we focus on the detailed investigation of the relation between synthesis and structural properties of homoepitaxial grown $SrTiO_3$ films in this small pressure regime between 10^{-2} and 10^{-1} mbars in which the change in propagation behaviour of the species abruptly takes place. As these films are grown with a variation in background pressure of only one order of magnitude, it is expected that the observed changes in thin film characteristics are dominated by variations in the composition of the plasma plume, while no significant differences in oxygen vacancy concentration are expected.

While we only present measurements that indirectly point to the role of the distribution and chemistry of plasma species, our results indicate a strong dependence of the film kinetic growth characteristics, morphology, and cation (non)stoichiometry on the ratio of oxidized and neutral species in the plasma plume. Thin films with varying thicknesses have been grown for specific deposition pressures and laser fluence conditions. The experimental results have enabled us to propose a model to describe in more detail the relation between the structural properties of the $SrTiO_3$ films and the controlled growth parameters. We suggest that sticking and mobility of species at the substrate surface are strongly related to its oxidation state, which is an intricate balance between oxygen from the target material, oxidation during the propagation towards the substrate by interactions with the oxygen background gas, and oxygen scavenging from the oxide substrate.

Two sets of $SrTiO_3$ thin film samples have been grown by PLD: the first series were grown at an absolute pressure of 0.01, 0.02, 0.04, 0.06, 0.08, and 0.1 mbars oxygen; for the second series we used a mixture of oxygen and argon, where the total pressure was kept at 0.08 mbars and partial pressures were 0.01, 0.02, 0.04, 0.06, 0.08 mbars of oxygen. In both cases, the growth temperature was kept constant at 710 °C.

A combined chemical and thermal treatment was applied to achieve a single TiO_2 termination of the STO substrates.[21] The laser fluence was set to 1.3 J/cm^2 with a laser repetition rate at 1 Hz, spot size of 2.3 mm^2, and a target-substrate distance of 50 mm. All films were monitored during growth using reflection high energy electron diffraction (RHEED) to study the growth kinetics, surface morphology, and in-plane crystal structure. Furthermore, by monitoring the time-dependent evolution of the specular spot intensity information is obtained about the kinetic growth characteristics. Based on RHEED oscillations, the growth rate is determined (in the absolute pressure range from 0.01 mbars to 0.1 mbars varying from 13 pulses per unit cell layer to 22 pulses per unit cell layer, respectively). For a fixed total pressure, the variation is much smaller as expected, see also Figures S1 and S2 of the supplementary material.[22] Subsequently, X-ray diffraction (XRD) was used for structural characterisation of the thin films, focussing on the changes in the out of

This article is copyrighted as indicated in the article. Reuse of AIP content is subject to the terms at: http://aplmaterials.aip.org/about/rights_and_permissions
Downloaded to IP: 130.89.45.179 On: Wed, 28 Oct 2015 08:42:35

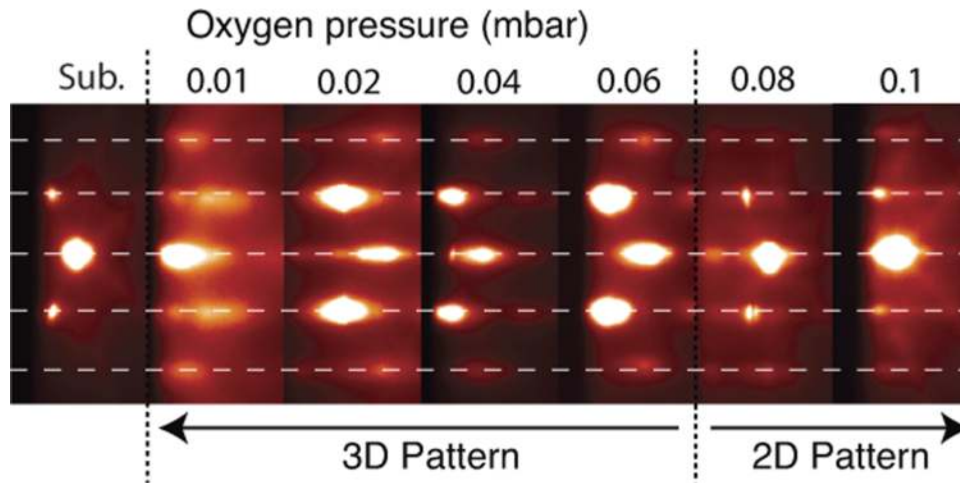

FIG. 1. RHEED diffraction patterns after each deposition of 100 monolayers of $SrTiO_3$ at indicated absolute oxygen pressures. The arrows indicate a transition in the type of pattern corresponding to a 3D pattern at lower pressures and a 2D pattern above 0.06 mbars.

plane lattice constant by performing $2\theta/\omega$ symmetrical scans around the (002) Bragg reflection of $SrTiO_3$ as this is the strongest out-of-plane reflection. Based on RHEED oscillations the growth rate is determined, which is translated to a total deposition time for growing 100 monolayers (ML). For a bulk lattice constant of 3.905 Å, this results in 39 nm thick films. A nonstoichiometry, associated with an increase in unit cell volume,[23] will therefore result in a thicker film. After growth, all films have been cooled down to room temperature with 50 °C/min at 100 mbars of oxygen pressure.

The corresponding RHEED diffraction patterns in the [01] direction after growth of 100 monolayers are shown in Figure 1. Patterns were taken after subsequent cool down to room temperature and at a base pressure of $\sim 10^{-7}$ mbars. On the outer left side, a typical diffraction pattern of a TiO_2 single terminated $SrTiO_3$ substrate surface is shown. To the right, diffraction patterns of $SrTiO_3$ films deposited at increasing pressures are shown. The most striking qualitative difference is the presence of a 3D or transmission pattern for growth pressures up to 0.06 mbars. Such 3D pattern is formed by dominant transmission electron diffraction through small surface asperities on a roughened surface, which was also confirmed by rocking the incident beam to ensure the fixed position of diffraction spots on the phosphorus screen. Differences in overall intensity between images are caused by a varying filament current or a small change in angle between sample and the grazing electron beam, resulting in a slightly changed diffraction condition affecting the individual spot intensity. The patterns at 0.08 and 0.1 mbars show clear 2D 0th-order spots, while for 0.1 mbars, Kikuchi lines are also visible, indicating a high degree of crystallinity. These 2D patterns are very similar to those of a typical (1×1) pattern of a single TiO_2-terminated $SrTiO_3$ substrate, indicating that the top surface is atomically flat.

An investigation into the in-plane position of the diffraction spots, as emphasised with the horizontal lines outlined to the substrate peak position, shows that for the films grown at highest pressure conditions, the surface structure is identical to the substrate. Even the relative intensity difference between the main and side spots shows qualitative resemblances to the substrate diffraction pattern. This weaker intensity of the side spots compared to the main specular spot has been reported to be the signature of a TiO_2 single terminated $SrTiO_3$ substrate.[24] Presumably, a mixed terminated substrate will show stronger side spots as a result of a difference in structure factor between strontium and titanium atoms.

Figure 2 shows the RHEED surface diffraction patterns in [01] direction after growth varying the oxygen partial pressure, similar to Figure 1. Indicated with the arrows is the transition from a 3D to 2D surface diffraction pattern for the films grown at, respectively, 0.06 mbars and 0.08 mbars oxygen partial pressure, a similar transition to the films grown at absolute oxygen pressure.

This article is copyrighted as indicated in the article. Reuse of AIP content is subject to the terms at: http://aplmaterials.aip.org/about/rights_and_permissions Downloaded to IP: 130.89.45.179 On: Wed, 28 Oct 2015 08:42:35

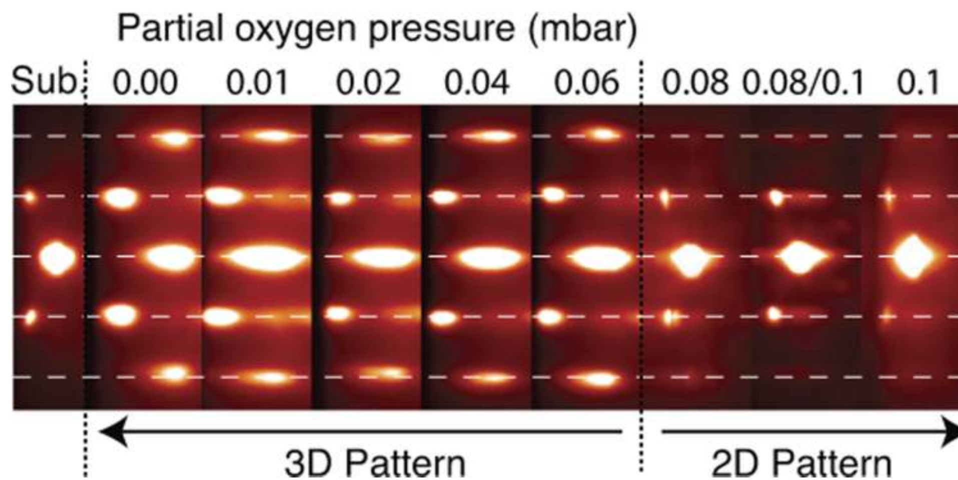

FIG. 2. RHEED diffraction patterns after each deposition of 100 monolayers of $SrTiO_3$ at indicated oxygen partial pressures, where the total pressure was kept at 0.08 mbars by adding Ar; the two right-most panels represent samples grown at a total pressure of 0.1 mbars. The arrows indicate a transition in the type of pattern corresponding to a 3D pattern at lower pressures and a 2D pattern above 0.06 mbars.

Next, we investigate the structural properties of the grown films. Figure 3 shows $2\theta/\omega$ symmetrical scans around the (002) Bragg reflection of $SrTiO_3$ for samples grown at absolute (a), and partial (b) oxygen background gas pressure from 10^{-2} to 10^{-1} mbars.

For the films grown at absolute background gas pressure, films grown at pressures of 0.01, 0.02 and 0.04 mbars show clear film peaks indicated with a red arrow. The corresponding lattice parameters for these pressures are respectively 3.927 ± 0.001 Å, 3.935 ± 0.001 Å, and 3.933 ± 0.001 Å. At 0.06 mbars, a striking transition is observed in the position of the film peak shifting towards the substrate peak, visible as a shoulder peak next to the substrate peak. For the film grown at 0.08 mbars, no distinguishable film peak is present. For the film grown at 0.1 mbars, a shoulder peak is again visible. The shift in peak position left from the substrate peak corresponds to an increase of the film c-axis with respect to the substrate and therefore to an increased unit cell volume. This is caused by nonstoichiometry, or point defects in the lattice. As for the film grown at 0.08 mbars the film is nearly indistinguishable from the substrate, this film is most stoichiometric. For all films, Kiessig fringes around the film peaks are observed resulting from the coherence between individual layers in the film and indicate high crystalline quality.

Figure 3(b) shows similar measurements for the films grown at oxygen partial pressures. As indicated, total pressure is kept at 0.08 mbars. The measurement indicated with 0.00 mbar represents the results on a sample grown at pure 0.08 mbars argon pressure. Deviating from the total pressure of 0.08 mbars, the top measurement is the result of a film grown at a total pressure of 0.1 mbars, with partial pressure of 0.08 mbars oxygen.

Unlike the films grown at absolute oxygen pressure, showing a more abrupt transition in film peak position with increasing pressure, a more gradual transition is observed for increasing partial pressure. The peak position increases towards the value of the substrate peak. For the films grown at 0.06 mbars and 0.08 mbars partial pressure, the film is nearly indistinguishable from the substrate. The film grown at 0.1 mbars shows again a clear shoulder. In all measurements, Kiessig fringes indicate a high degree of crystallinity. Again, as the increase in unit cell volume is the result of point defects in the film lattice, the increase in oxygen partial pressure results in a decrease in defects related to an improved stoichiometry up until a nearly stoichiometric film grown at 0.06 mbars oxygen partial pressure.

For a further quantification of the out-of-plane XRD scans, measurements are simulated and fitted using the model given by Stepanov (Stepanov X-ray server).[25] The main focus of this investigation is the accurate determination of the position of the film peak and the lattice parameter of the film. Furthermore, from the fits of the Kiessig fringes the film thickness was determined. The results

This article is copyrighted as indicated in the article. Reuse of AIP content is subject to the terms at: http://aplmaterials.aip.org/about/rights_and_permissions
Downloaded to IP: 130.89.45.179 On: Wed, 28 Oct 2015 08:42:35

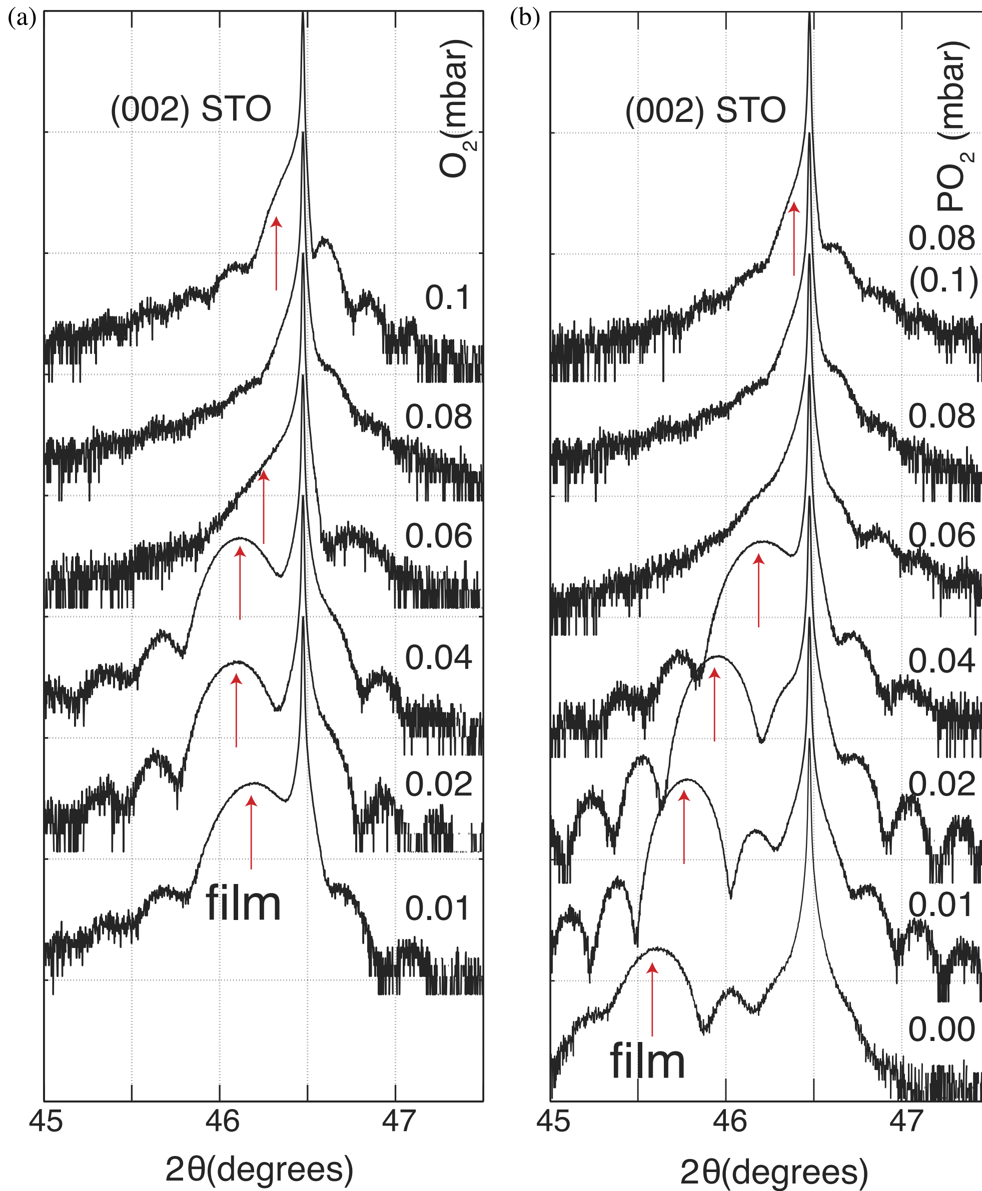

FIG. 3. XRD $2\theta/\omega$ scans for $SrTiO_3$ film grown at absolute (a) and partial (b) oxygen pressure around the (002) Bragg reflection of the $SrTiO_3$ substrate. Film peaks are indicated with the red arrows, where the peak positions for the films grown in oxygen partial pressure show striking trends with increasing pressure.

of the simulations and relevant parameters are given in Table I. See the supplementary material for details.[22] For most films, a simple one-layer system with high crystallinity, a specifically chosen d-spacing and thickness would result in fairly accurate simulations. Only for the film grown in pure argon (pO_2 = 0.00), the overall crystallinity simulated with the so called Debye-Waller coefficient of 0.4 strongly deviated from 1, or perfect crystallinity.

Small deviations in the simulations with the respect to the measurements were corrected by the introduction of an extra thin second layer in between (†) or on top (‡) of the film, characterised by a low crystallinity, large roughness, and deviating lattice constant. Although the values for the chosen physical parameters are likely to be unreliable, as these parameters have interchangeable effects on the simulations, the qualitative presence of such a second layer could be very well explained in the form of a layer representing slight surface roughening, which is the case for all films. Nonetheless, due to their limited relevance, no further attention will be given to this extra top layer.

This article is copyrighted as indicated in the article. Reuse of AIP content is subject to the terms at: http://aplmaterials.aip.org/about/rights_and_permissions Downloaded to IP: 130.89.45.179 On: Wed, 28 Oct 2015 08:42:35

TABLE I. Film (002) Bragg reflection position shift as percentage of the substrate da/a (%) ($SrTiO_3$ c-axis is 3.905 Å), and corresponding film thickness d (Å). Note: (∗) A Debye-Waller coefficient of 0.4 was used, likely corresponding to a strong decrease in crystallinity. (†) A monolayer thick interface layer was introduced between film and substrate with deviating d-spacing. (‡) A 10 Å thin layer with deviating d-spacing on top of the film was used to correct deviations between simulation and measurements.

pO_2 (mbar)	da/a (%)	d (Å)
0.00*	1.9	330
0.01	1.5	350
0.02	1.2	350
0.04	0.6	290
0.06†	0.02	370
0.08‡	0.05	380
0.08/010‡	0.06	390
010‡	0.14	390

Summarising, the outcome of these simulations is that with increasing partial pressure the d-spacing increases and for the film grown at 0.06 mbars oxygen partial pressure the d-spacing matches the substrate, while further increasing the pressure the d-spacing increases again. Assuming that the substrate material represents stoichiometric $SrTiO_3$ the 0.06 mbars film material should also be stoichiometric. Furthermore, the thickness determined from these simulations is deviating from the original aim of a 100 ML (39 nm) thick films based on the first RHEED oscillations. Based on additional experiments varying the total thickness (see Fig. S4 of the supplementary material[22]), a $SrTiO_3$ film is initially formed with nearly perfect stoichiometry and, therefore, no significant change in c-axis. This would make these initial layers indistinguishable from the substrate for XRD. After a certain amount of layers, the film stoichiometry changes, forming the second layer with an increased c-axis and corresponding thickness obtained from the Kiessig fringe periodicity.

Finally, we studied the dependence of the stoichiometry on the laser fluence. In Figure 4, XRD scans are shown of samples deposited using different laser fluences (maintaining the same spot size). Figure 4(a) shows samples grown at an absolute oxygen pressure of 0.01 mbars. Figure 4(b) shows films grown at a oxygen partial pressure of 0.01 mbars with a total pressure of 0.08 mbars. When depositing in the ballistic regime, the laser fluence did affect the stoichiometry of the films, as can be concluded from the position of the main film peak, whereas when depositing above the diffusive threshold the peak position did not change and therefore the stoichiometry remains constant.

The results from the growth and structural investigation of homoepitaxially grown $SrTiO_3$ films show a significant dependence of film characteristics on the background gas pressure conditions. Regarding film structural characterisation, a strong dependence of the c-axis of the film as function of pressure is observed. Regarding growth kinetics, with increasing pressure, layer-by-layer growth was more strongly maintained, indicating improved film smoothness, supported by the surface diffraction patterns which show a similar 3D to 2D transition. Kinetically, improved film smoothness implies an improved diffusion, or mobility of particles on the substrate.

Current growth models suggest a pressure dependent diffusion activation energy, which increases with increasing pressure, in specifically the pressure regime focus of this research between 10^{-2} and 10^{-1} mbars. It is assumed that the increase of activation energy with increasing pressure is the result of the thermalisation of arriving species, which happens in exactly this pressure regime. Subsequently, relaxation is slower at higher pressures, resulting in surface roughening. The model therefore assumes that just the changing kinetics of arriving species affects the relaxation on the substrate.

This work points to an additional important parameter, namely, the oxidation of species in the plasma. When looking at films grown in absolute pressure, surface smoothening is observed with increasing pressures due to enhanced diffusivity related to the oxidation of the arriving species.

This article is copyrighted as indicated in the article. Reuse of AIP content is subject to the terms at: http://aplmaterials.aip.org/about/rights_and_permissions Downloaded to IP: 130.89.45.179 On: Wed, 28 Oct 2015 08:42:35

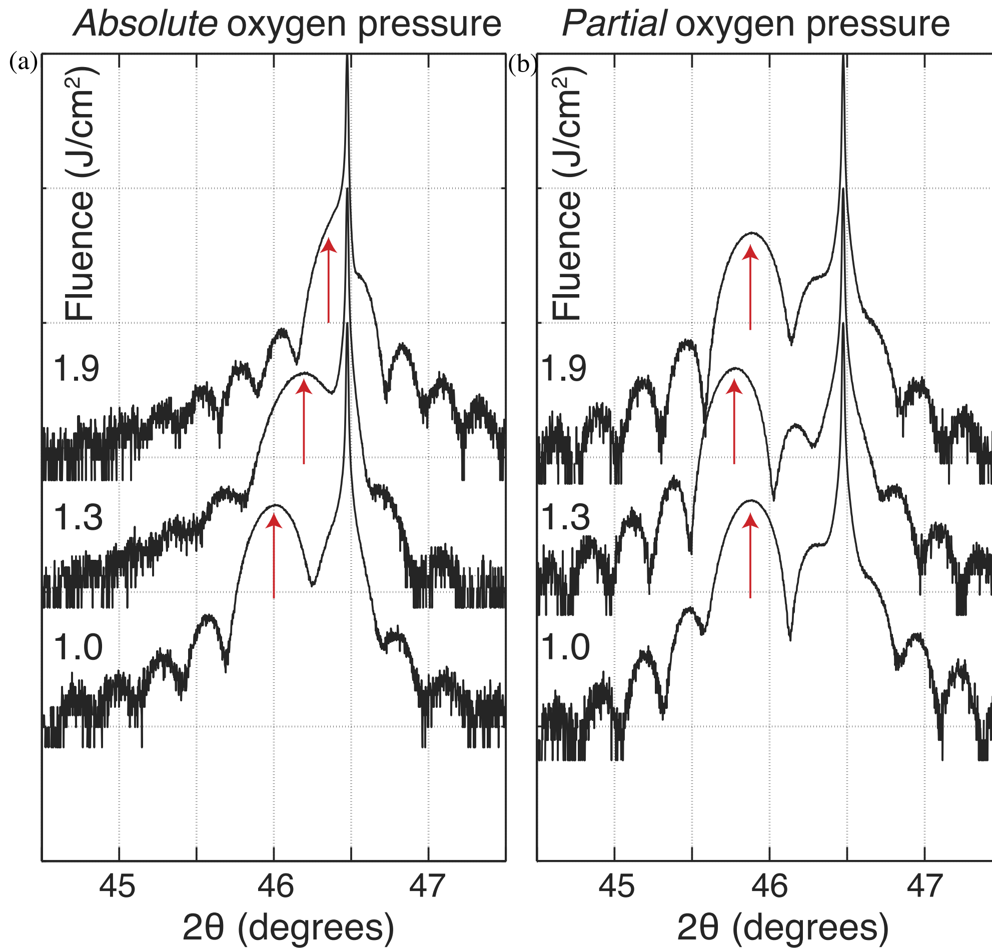

FIG. 4. XRD θ–2θ scans of films grown at different laser fluences at 0.01 mbars absolute (a) and partial pressure (b).

The results on the samples grown at partial pressures where a similar transition in the surface morphology is observed, independent of the kinetic energy of the species, support the oxidation model. What is overlooked in the kinetic model is the nature of species that arrive on the growth surface and its subsequent diffusion and relaxation behaviour.

From the XRD simulation we derived the film thicknesses and observed that they are deviating from the estimated thickness from the RHEED oscillations, with the exception of the film grown at highest pressure where the thickness estimated from both XRD as well as RHEED agree. The question is what is causing the deviating film thickness based on the Kiessig fringe spacing. The Kiessig fringes originate from the coherence between individual monolayers within a finite size film, which has a clear interface with the substrate. This interface results naturally when a density difference between film and substrate is present, for example caused by a change in stoichiometry or more generally for films with increased d-spacing. The film grown at 0.06 mbars is nearly perfect with respect to the substrate, but Kiessig fringes are still visible likely due to a single interfacial monolayer with deviating d-spacing resulting in a phase change between the film lattice and the substrate lattice.[26]

As mentioned before, in the supplementary material (Fig. S4),[22] we describe experiments performed varying the thickness of the $SrTiO_3$ overlayer. From these measurements we conclude that an initial stoichiometric layer is stabilised, even when nominally depositing under conditions when non-stoichiometry would be expected due to lack of oxygen. The stabilisation apparently occurs with the substrate as the source of oxygen in the picture of oxidation of surface species being the most important to determine sticking as well as diffusivity. In addition, the process of bulk oxygen

This article is copyrighted as indicated in the article. Reuse of AIP content is subject to the terms at: http://aplmaterials.aip.org/about/rights_and_permissions
Downloaded to IP: 130.89.45.179 On: Wed, 28 Oct 2015 08:42:35

supply is limited by the surface morphology as well as bulk diffusion of oxygen leading to a finite interfacial layer thickness as is seen in both XRD (as "missing" thickness) as well as RHEED oscillations for each individual sample, pointing to a thickness of this layer somewhere between 7 and 11 monolayers.

Finally, the fact that the stoichiometry observed in films grown at absolute oxygen pressure does depend on the laser fluence and in the case of partial pressures (with a total pressure kept at 0.08 mbars) there was no fluence dependence agrees with the oxidation model. The fluence would most likely affect the elemental specific spatial distribution in the ballistic regime because of mass differences. This effect is suppressed by the plume confinement in the diffusive regime.

Our overall conclusion from the XRD and RHEED analyses of films grown under different oxidising ambient conditions is that both stoichiometry as well as surface diffusivity were controlled by the oxidation of arriving species and not so much their kinetic energy. We have indirect evidence that for PLD the oxidation can be controlled within the plasma plume before species arrive on the growth surface, in addition to the observed oxygenation by substrate or target oxygen. We expect the better understanding of PLD thin film growth using oxides will lead to improved, better controlled thin films. This observation will have broader implications on the interpretation of observed growth behaviour for various thin film techniques.

This research is supported by the Dutch Technology Foundation STW which is part of the Netherlands Organization for Scientific Research (NWO) and partly funded by the Ministry of Economic Affairs (project number 10760).

[1] Y. Kozuka, Y. Hikita, C. Bell, and H. Y. Hwang, "Dramatic mobility enhancements in doped $SrTiO_3$ thin films by defect management," Appl. Phys. Lett. **97**(1), 2107 (2010).

[2] J. Son, P. Moetakef, B. Jalan, O. Bierwagen, N. J. Wright, R. Engel-Herbert, and S. Stemmer, "Epitaxial $SrTiO_3$ films with electron mobilities exceeding 30 000 cm^2 V^{-1} s^{-1}," Nat. Mater. **9**(6), 482–484 (2010).

[3] M. L. Scullin, J. Ravichandran, C. Yu, M. Huijben, J. Seidel, A. Majumdar, and R. Ramesh, "Pulsed laser deposition-induced reduction of $SrTiO_3$ crystals," Acta Mater. **58**(2), 457–463 (2010).

[4] E. Breckenfeld, R. Wilson, J. Karthik, A. R. Damodaran, D. G. Cahill, and L. W. Martin, "Effect of growth induced (non) stoichiometry on the structure, dielectric response, and thermal conductivity of $SrTiO_3$ thin films," Chem. Mater. **24**(2), 331–337 (2012).

[5] M. P. Warusawithana, C. Richter, J. A. Mundy, P. Roy, J. Ludwig, S. Paetel, T. Heeg, A. A. Pawlicki, L. F. Kourkoutis, M. Zheng, M. Lee, B. Mulcahy, W. Zander, Y. Zhu, J. Schubert, J. N. Eckstein, D. A. Muller, C. S. Hellberg, J. Mannhart, and D. G. Schlom, "$LaAlO_3$ stoichiometry is key to electron liquid formation at $LaAlO_3/SrTiO_3$ interfaces," Nat. Commun. **4**, 2351 (2013).

[6] H. W. Jang, A. Kumar, S. Denev, M. D. Biegalski, P. Maksymovych, C. W. Bark, C. T. Nelson, C. M. Folkman, S. H. Baek, N. Balke, C. M. Brooks, D. A. Tenne, D. G. Schlom, L. Q. Chen, X. Q. Pan, S. V. Kalinin, V. Gopalan, and C. B. Eom, "Ferroelectricity in strain-free $SrTiO_3$ thin films," Phys. Rev. Lett. **104**(19), 197601 (2010).

[7] T. Ohnishi, K. Shibuya, T. Yamamoto, and M. Lippmaa, "Defects and transport in complex oxide thin films," J. Appl. Phys. **103**(10), 103703 (2008).

[8] S. Wicklein, A. Sambri, S. Amoruso, X. Wang, R. Bruzzese, A. Koehl, and R. Dittmann, "Pulsed laser ablation of complex oxides: The role of congruent ablation and preferential scattering for the film stoichiometry," Appl. Phys. Lett. **101**(13), 131601 (2012).

[9] G. Koster, G. J. H. M. Rijnders, D. H. A. Blank, and H. Rogalla, "Imposed layer-by-layer growth by pulsed laser interval deposition," Appl. Phys. Lett. **74**(24), 3729 (1999).

[10] D. Blank, G. Koster, and G. Rijnders, "Epitaxial growth of oxides with pulsed laser interval deposition," J. Cryst. Growth **211**, 98–105 (2000).

[11] C. Xu, S. Wicklein, A. Sambri, S. Amoruso, M. Moors, and R. Dittmann, "Impact of the interplay between nonstoichiometry and kinetic energy of the plume species on the growth mode of $SrTiO_3$ thin films," J. Phys. D: Appl. Phys. **47**(3), 034009 (2014).

[12] G. Liu and Q. Lei, "Stoichiometry of $SrTiO_3$ films grown by pulsed laser deposition," Appl. Phys. Lett. **100**, 202902 (2012).

[13] B. Dam, J. Rector, and J. Johansson, "Mechanism of incongruent ablation of $SrTiO_3$," J. Appl. Phys. **83**(6), 3386–3389 (1998).

[14] T. Ohnishi, M. Lippmaa, and T. Yamamoto, "Improved stoichiometry and misfit control in perovskite thin film formation at a critical fluence by pulsed laser deposition," Appl. Phys. Lett. **87**, 241919 (2005).

[15] S. Amoruso and A. Sambri, "Propagation dynamics of a LaMnO laser ablation plume in an oxygen atmosphere," J. Appl. Phys. **100**, 013302 (2006).

[16] D. Geohegan, "Physics and diagnostics of laser ablation plume propagation for high-Tc superconductor film growth," Thin Solid Films **220**, 138–145 (1992).

[17] M. Strikovski and J. H. Miller, "Pulsed laser deposition of oxides: Why the optimum rate is about 1 Å per pulse," Appl. Phys. Lett. **73**(12), 1733 (1998).

[18] J. Boschker, E. Folven, Å. Monsen, E. Wahlstrøm, J. Grepstad, and T. Tybell, "Consequences of high ad-atom energy during pulsed laser deposition of $La_{0.7}Sr_{0.3}MnO_3$," Cryst. Growth Des. **12**, 562–566 (2012).

This article is copyrighted as indicated in the article. Reuse of AIP content is subject to the terms at: http://aplmaterials.aip.org/about/rights_and_permissions
Downloaded to IP: 130.89.45.179 On: Wed, 28 Oct 2015 08:42:35

[19] P. Willmott, R. Herger, C. Schlepütz, and D. Martoccia, “Energetic surface smoothing of complex metal-oxide thin films,” Phys. Rev. Lett. **96**, 176102 (2006).
[20] K. Sturm and H.-U. Krebs, “Quantification of resputtering during pulsed laser deposition,” J. Appl. Phys. **90**(2), 1061 (2001).
[21] G. Koster, B. L. Kropman, G. J. H. M. Rijnders, D. H. A. Blank, and H. Rogalla, “Quasi-ideal strontium titanate crystal surfaces through formation of strontium hydroxide,” Appl. Phys. Lett. **73**(20), 2920 (1998).
[22] See supplementary material at http://dx.doi.org/10.1063/1.4926933 for time dependent RHEED intensity recorded during growth, XRD fitting results and additional experiments varying the thickness of the $SrTiO_3$ films.
[23] B. Jalan, P. Moetakef, and S. Stemmer, “Molecular beam epitaxy of $SrTiO_3$ with a growth window,” Appl. Phys. Lett. **95**, 032906 (2009).
[24] G. Koster, G. Rijnders, D. H. A. Blank, and H. Rogalla, “Surface morphology determined by (001) single-crystal $SrTiO_3$ termination,” Physica C **339**, 215–230 (2000).
[25] S. A. Stepanov, E. A. Kondrashkina, R. Köhler, D. V. Novikov, G. Materlik, and S. M. Durbin, “Dynamical x-ray diffraction of multilayers and superlattices: Recursion matrix extension to grazing angles,” Phys. Rev. B **57**(8), 4829–4841 (1998).
[26] J. M. Lebeau, R. Engel-Herbert, B. Jalan, J. Cagnon, P. Moetakef, S. Stemmer, and G. B. Stephenson, “Stoichiometry optimization of homoepitaxial oxide thin films using x-ray diffraction,” Appl. Phys. Lett. **95**, 142905 (2009).

This article is copyrighted as indicated in the article. Reuse of AIP content is subject to the terms at: http://aplmaterials.aip.org/about/rights_and_permissions
Downloaded to IP: 130.89.45.179 On: Wed, 28 Oct 2015 08:42:35